J. Fluid Mech. (1989), *vol.* 204, *pp.* 245–262
Printed in Great Britain

Active stabilization of compressor surge

By J. E. FFOWCS WILLIAMS AND X. Y. HUANG
Department of Engineering, University of Cambridge, Trumpington Street, Cambridge, CB2 1PZ, UK

(Received 25 January 1988)

This paper describes the stabilization of compressor surge by an active method. It is known that surge follows when small disturbances grow in an unstable compression system, and that small growth can be modelled through a linear stability analysis. An active element is here introduced to counter any tendency to instability and the control law governing the active stabilizer is determined from linear theory. We follow precisely the suggestion put forward by Epstein *et al.* (1986) and verify that their theory conforms to practice. The theory is verified in an experiment on a compression system whose plenum volume is controlled. Suppression of the flow instability was achieved by switching on the controller and the compressor was made to operate stably on a part of its characteristic beyond the nature stall line. Furthermore the controlled compressor is much more resilient to external disturbances than is the natural case. The controller is even effective on deep surge – a feature of great interest but hardly predictable from the Epstein *et al.* initiative for this kind of study.

1. Introduction

The mean pressure rise across a compressor rotor revolving at steady speed is characterized by the pressure rise versus throughflow curve. This characteristic has a maximum, near the point corresponding to incipient stall conditions where flow is becoming detached from the rotor surfaces. The angle of incidence onto the sections is reduced by increasing the throughflow, so that the right-hand side of the characteristic curve marks a region where the flow tends to be stable and the slope of the pressure/throughflow line is negative. On the left of the peak pressure points tends to lie the unstable region where the flow is rough and unsteady.

The pressure delivered by the compressor must of course drive the flow onward through the 'throttle' that controls the throughflow rate, the higher the pressure the higher the flow, the precise form of the throttle pressure versus throughflow characteristic depending on the throttle area. Three typical cases are illustrated in figure 1, the mean flow through the compressor/throttle system being set at the points where the compressor and throttle characteristics meet. Case 1 and case 2 in that illustration correspond to stable compressor operation while case 3 is unstable. In that case there are large-amplitude oscillations in the compressor delivery pressure (Emmons, Pearson & Grant 1955; Greitzer 1976) and that system instability is known as surge. Although the detailed mechanism of surge is complex, its principal features are contained in a beautifully simple model (Greitzer 1981). The unsteady behaviour of the compressor system (consisting of a compressor, a duct, a plenum volume and a throttle) is akin to that of a Helmholtz resonator in which the compressor is an energy source and the throttle a damper. The inertia of the fluid in the duct and the 'springiness' of the compressible fluid in the plenum constitute the

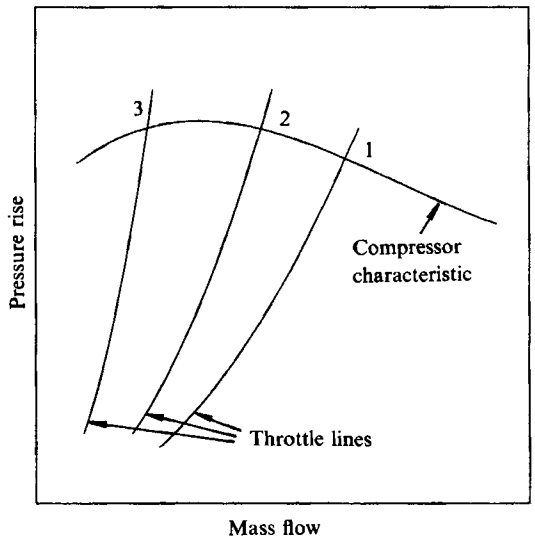

FIGURE 1. Typical characteristics of a compression system.

resonant elements. When the oscillation receives more energy from the compressor than is dissipated in the throttle then any small perturbation in the flow will grow, initially exponentially with time and eventually developing into a large-amplitude oscillation limited by the nonlinear characteristics of the system. The stability of a compression system to small perturbations is critical to whether or not surge will occur, and the onset of surge can be predicted by a linear stability analysis (Emmons *et al.* 1955; Stenning 1980). This linear model, if valid, implies that compressor surge will be suppressed by the active technique described by Epstein, Ffowcs Williams & Greitzer (1986). The main strategy of this control method is that the pressure fluctuation in the plenum is monitored, the signal phase-shifted and amplified to drive an element that varies the volume of the plenum. By means of the unsteady but controlled plenum volume, the natural balance between throttle and compressor flows is distorted; a controlled perturbation can alter the energy fed in by the compressor, change the dissipative energy through the throttle, and contribute to the oscillation energy directly, the precise effect depending on how the feedback signals are processed.

In this paper, we demonstrate experimentally that compressor surge is indeed suppressed by the feedback system suggested by Epstein *et al.* (1986).

2. Stability of the compression system

2.1. *Compression system used in the experiments*

Our compression system consists of a centrifugal compressor (Holset type H1A) producing a pressure rise while delivering mass flow to a plenum. The discharge is through a duct of small diameter and throttled by a flow restricting valve. The compression system is at the ambient pressure at the compressor inlet and downstream of the throttle. A schematic illustration is shown in figure 2. During the experiments the compressor was operated over a range of speeds between 40000 and 80000 r.p.m.

The equations governing the dynamics of this compression system are the

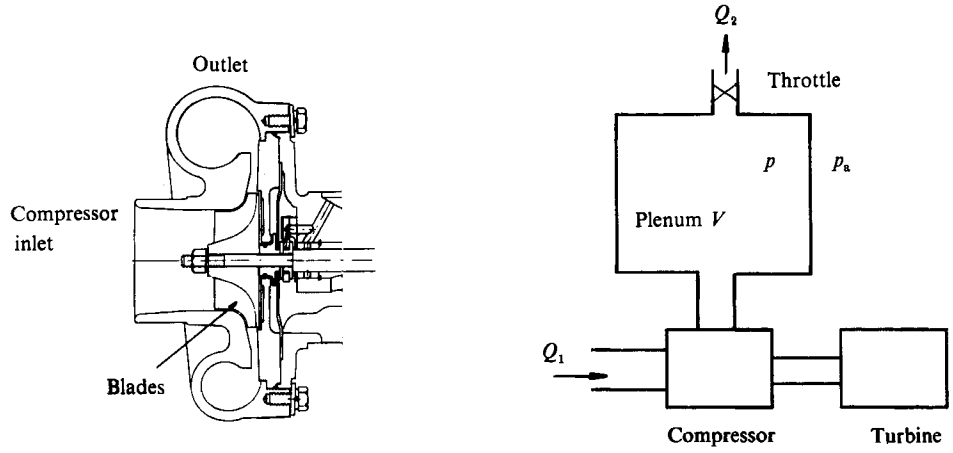

FIGURE 2. The compressor and a schematic illustration of the compression system used in the experiments.

particular cases of equations (11), (12) and (13) in Greitzer (1976). The detailed form has been found from experiment (Huang 1988) to be

$$\chi_c \frac{dQ_1}{dt} = f_1(Q_1) - (p - p_a) - \sigma_c(Q_1 - \bar{Q}_1), \tag{1a}$$

$$\frac{V}{a^2}\frac{dp}{dt} = Q_1 - Q_2, \tag{1b}$$

$$\chi_t \frac{dQ_2}{dt} = (p - p_a) - f_2(Q_2). \tag{1c}$$

The term $\chi_c(dQ_1/dt)$ represents the inertia of the flow in the compressor; χ_c is roughly proportional to the ratio of compressor length to diameter. χ_t is a similar parameter for the throttle duct. $\sigma_c(Q_1 - \bar{Q}_1)$ is an experimentally determined term prescribing the flow resistance in the compressor duct.

In steady operation at constant mass flow rate $\bar{Q}_1$ the pressure rise $f_1(\bar{Q}_1)$ produced by the compressor is a characteristic function of that mass flow. We have measured this function with a special plenum whose volume was so small that the system was free from surge in our measured mass flow range. The results are shown in figure 3, together with an approximate empirical curve-fit to the data:

$$\begin{aligned}\text{mean pressure rise} &= f_1(\bar{Q}_1)\\ &= \tfrac{1}{2}\rho U^2\{0.045 \arctan[120(\bar{\phi}_1 - 0.052)] + 1.18\\ &\quad + 0.85\bar{\phi}_1 - 7.2\bar{\phi}_1^2 + 4.7\bar{\phi}_1^3\}.\end{aligned} \tag{2}$$

$\bar{\phi}_1 = \bar{Q}_1/(\rho A_c U)$ is the non-dimensional mass flow rate, where U is the speed of the compressor blade tip, ρ is the mean air density (a constant in the experiment) and A_c the cross-sectional area of the inlet duct.

In steady operation, the pressure drop $f_2(\bar{Q}_2)$ across the throttle is a function of the mass flow rate $\bar{Q}_2$. Under the conditions of the experiments, this function has been found to be

$$f_2(\bar{Q}_2) = S\bar{Q}_2^2, \tag{3}$$

where S is a coefficient depending on the throttle area A_t.

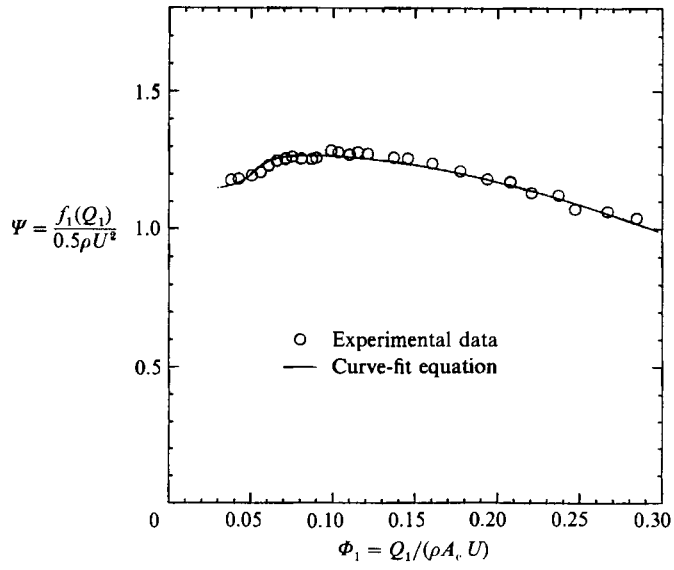

FIGURE 3. Characteristic of the compressor used in the experiment and the curve fitting formula in equation (2).

We found the Helmholtz resonance frequency for our system to be $\omega_H = 2\pi \times 37\ s^{-1}$ by measuring the system response to a pressure impulse. It also can be calculated from the usual formula $\omega_H = a[1/(V\chi_c)]^{\frac{1}{2}}$, taking measured values for the plenum volume $V = 5.5 \times 10^{-3}\ m^3$, the parameter of the compressor duct $\chi_c = 3.9 \times 10^3\ m^{-1}$ and the speed of sound $a = 340$ m/s. We have ignored the inertia of the flow in the throttle which is small in our experiment.

We non-dimensionlize the mass flow rate using the quantity $\rho A_c U$, the pressure using $\frac{1}{2}\rho U^2$ and the time t using the characteristic time $1/\omega_H$, to obtain the non-dimensional governing equations

$$\left.\begin{aligned} \frac{d\phi_1}{d\tau} &= B[\Psi(\phi_1) - P] - \mu(\phi_1 - \bar{\phi}_1), \\ \frac{dP}{d\tau} &= \frac{\phi_1 - \phi_2}{B}, \\ \frac{d\phi_2}{d\tau} &= \lambda B[P - T(\phi_2)], \end{aligned}\right\} \tag{4}$$

where

$$\phi_1 = \frac{Q_1}{\rho A_c U}, \quad \phi_2 = \frac{Q_2}{\rho A_c U}, \quad P = \frac{p - p_a}{\frac{1}{2}\rho U^2}, \quad \Psi = \frac{f_1(Q_1)}{\frac{1}{2}\rho U^2}, \quad T = \frac{f_2(Q_2)}{\frac{1}{2}\rho U^2}, \quad \tau = \omega_H t,$$

$$B = \frac{\frac{1}{2}U}{\omega_H A_c \chi_c}, \quad \mu = \frac{\sigma_1}{\omega_H \chi_c}, \quad \lambda = \frac{\chi_c}{\chi_t}.$$

2.2. *Linearized stability analysis*

To find whether the system is stable or unstable, we follow established convention and examine its response to small perturbations when operating at a given condition. With given mean values $\bar{\phi}_1 = \bar{\phi}_2 = \bar{\phi}$, $\bar{P} = \Psi(\bar{\phi}_1) = T(\phi_2)$, we set $\phi_1 = \bar{\phi} + \delta\phi_1$,

$\phi_2 = \bar{\phi} + \delta\phi_2$, $P = \bar{P} + \delta P$, $\Psi = \Psi(\bar{\phi}_1) + \Psi'\delta\phi_1$ and $T = \bar{P} + T'\delta\phi_2$ to arrive at the linear equations governing small-amplitude operation:

$$\left.\begin{aligned} \frac{\mathrm{d}\delta\phi_1}{\mathrm{d}\tau} &= B(\Psi'\delta\phi_1 - \delta P) - \mu\delta\phi_1, \\ \frac{\mathrm{d}\delta P}{\mathrm{d}\tau} &= \frac{\delta\phi_1 - \delta\phi_2}{B}, \\ \frac{\mathrm{d}\delta\phi_2}{\mathrm{d}\tau} &= \lambda B(\delta P - T'\delta\phi_2). \end{aligned}\right\} \tag{5}$$

These equations have solutions of the form $\mathrm{e}^{s\tau}$, for which (5) corresponds to the characteristic equation

$$s^3 + a_2 s^2 + a_1 s + a_0 = 0, \tag{6}$$

where

$$a_0 = \lambda(BT' + \mu - B\Psi'), \quad a_1 = 1 + \lambda + B\lambda T'(\mu - B\Psi'), \quad a_2 = \lambda BT' + \mu - B\Psi'.$$

The Routh–Hurwitz stability criterion (Drof 1980) gives necessary and sufficient conditions for the real parts of all roots of (6) to be negative as

$$a_0 > 0, \quad a_2 > 0, \quad a_1 a_2 > a_0. \tag{7}$$

These constraints define the stable range of our compression system. By substituting the measured values and the functions into (7), the linear instability point at which the stability conditions (7) will just be broken and the compression system will 'surge' can be predicted. We define the throttle characteristic corresponding to that instability point as the surge boundary.

We carried out an experiment to measure the surge onset point and compared the measured result with that predicted using (7). Figure 4 shows that the predicted result is satisfactorily close to the experimental result.

2.3. *Numerical evaluation and surge observation*

It is known (Emmons *et al.* 1955; Greitzer 1976) that when small fluctuations of the pressure and mass flow can grow in a compression system, they will finally develop into a limit cycle which makes the operating point (determined by the average pressure and mass flow rates) leave the original compressor characteristic; the compressor is then in surge. In that limit cycle, the oscillation amplitudes of the pressure and mass flow rate are relatively large and the oscillation frequency is usually lower than that of the most unstable small-amplitude fluctuations. Surge is limited by the nonlinear characteristics of the compressor and throttle. We have carried out a numerical calculation to solve equation (4) at the surge onset point and to observe qualitatively the transient behaviour as the weak fluctuations develop into surge. We agree that the nonlinear model is extremely heuristic – but nevertheless we think it is interesting enough to include. The experimental curve-fit function (2) was used as the compressor characteristic when the non-dimensional mass flow rate $\phi_1 > 0.04$, while in the range $\phi_1 < 0.04$, we used the parabola (Hansen Jørgensen & Larsen 1981), $1.1 + 32\phi_1^2$, the two curves being connected smoothly. The calculated results are illustrated in figure 5(*a*) by plotting the variation of the pressure P with time τ. We see that the pressure leaves its early unsteady stage when the oscillation amplitudes are still very small and settles into the amplitude-limited oscillations within a time of about 2–3 periods. The surge frequency is 89% lower than the Helmholtz resonance frequency in this numerical simulation. We have observed this system transient behaviour in our experiment by recording the

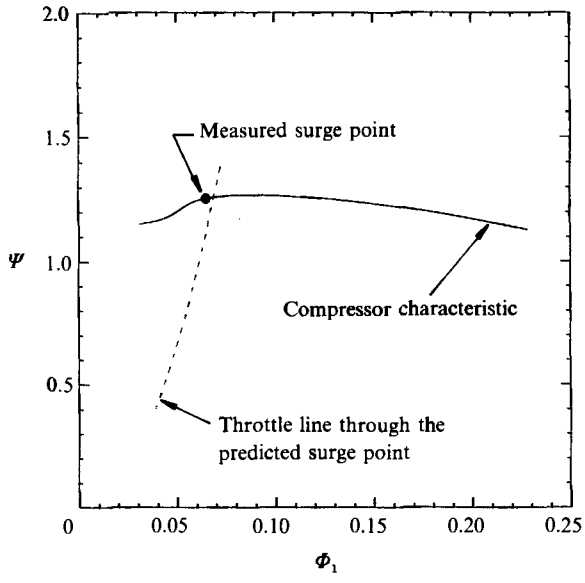

FIGURE 4. Experimental and predicted (by equation (7)) surge boundaries.

pressure fluctuation trace in the plenum; this is shown in figure 5(*b*). Before the onset of surge, the oscillation amplitudes were very small and were nearly submerged in the ever-present noise of the system. The surge frequency was found to be 65% lower than the Helmholtz resonance frequency.

3. The compression system with a controlled plenum

We now introduce a controller consisting of a surface A_3 which is part of a mass–spring system responding to the unsteady pressure fluctuation in the plenum and an externally induced control force; its displacement ξ produces a volumetric change $A_3\xi$ in the plenum. The mass stored in the plenum is thus changed by $\rho A_3\xi$ approximately. The displacement ξ is assumed to be proportional to the driving force, since the inertia of our surface A_3 is negligible in comparison with the spring stiffness at the frequencies in our experiment. The control force is generated by a feedback system which processes the signal detected by a pressure sensor located in the plenum. The whole system is schematically illustrated in figure 6(*a*). Based on that model, an experimental device was arranged, shown in figure 6(*b*), in which a loudspeaker implemented the surface A_3. The dynamic equations of the system are modified by the controller, from equation (1) to the following:

$$\chi_c \frac{dQ_1}{dt} = f_1(Q_1) - (p - p_a) - \sigma_c(Q_1 - \bar{Q}_1), \tag{8a}$$

$$\frac{V}{a^2}\frac{dp}{dt} = Q_1 - Q_2 - \underline{A_3\rho\frac{d\xi}{dt}}, \tag{8b}$$

$$\chi_t \frac{dQ_2}{dt} = (p - p_a) - f_2(Q_2), \tag{8c}$$

$$\underline{\xi = \frac{1}{K}(A_3 + C)(p - p_a)}. \tag{8d}$$

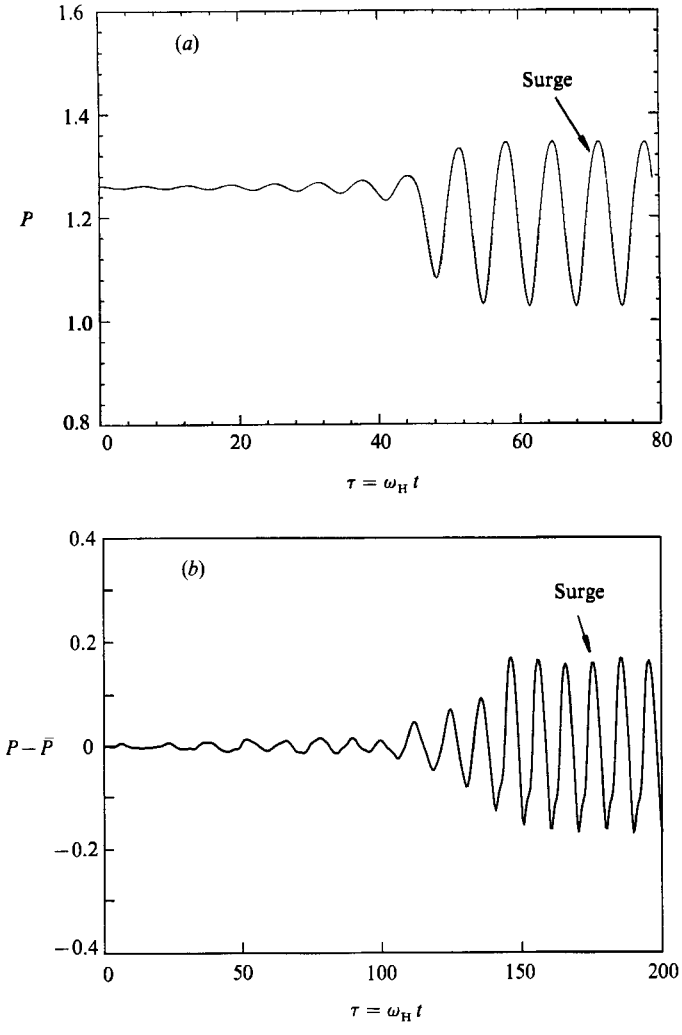

FIGURE 5. (*a*) Numerical simulation of the transient process as the small-amplitude pressure oscillations grows into surge. (*b*) A typical pressure trace recorded in the experiment at the point of surge onset.

The terms underlined represent the controller action. We have chosen to represent the controller as a variable area, C, though this is admittedly somewhat arbitrary. C is actually some temporal operator assumed to be independent of response amplitude. Equation (8) can be rearranged in non-dimensional form

$$\left.\begin{aligned} \frac{\mathrm{d}\phi_1}{\mathrm{d}\tau} &= B[\Psi(\phi_1)-P]-\mu(\phi_1-\bar{\phi}_1), \\ \frac{\mathrm{d}P}{\mathrm{d}\tau} &= \frac{\phi_1-\phi_2}{B}-(\eta+Z_\xi)\frac{\mathrm{d}P}{\mathrm{d}\tau}, \\ \frac{\mathrm{d}\phi_2}{\mathrm{d}\tau} &= \lambda B[P-T(\phi_2)], \end{aligned}\right\} \tag{9}$$

where $\eta = (\rho a^2 A_3^2/VK)$, $Z_\xi = (\rho a^2 A_3/VK)C$ (our operator Z_ξ is equivalent to Z_ξ/M^2 defined by Epstein *et al.* 1986); other parameters are the same as those in (4).

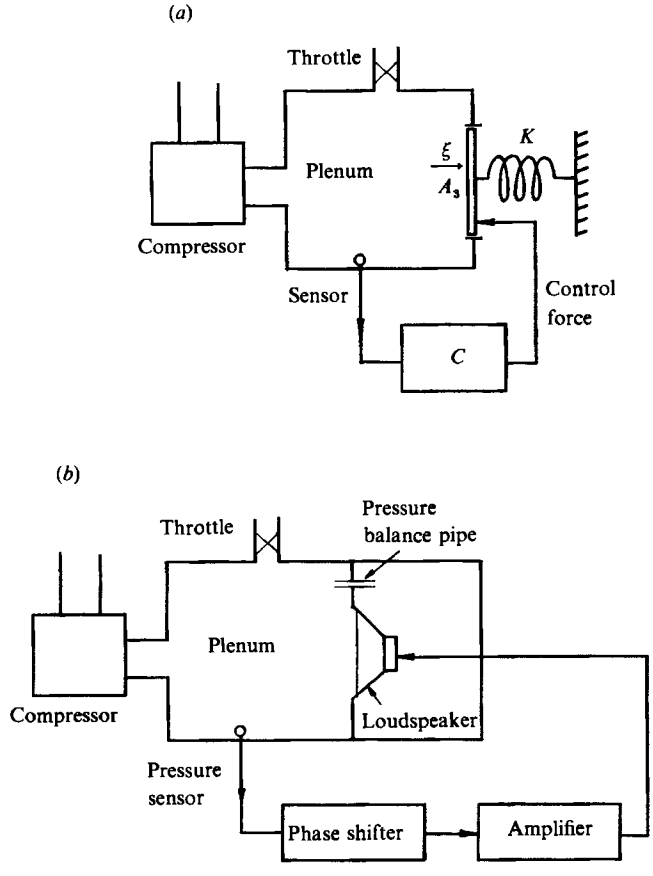

FIGURE 6. (a) Model of the compression system with a controlled plenum. (b) Geometry of the compression system with the controller used in the experiments.

Two new terms have been introduced into the governing equations by the controller. The term $\eta(\mathrm{d}P/\mathrm{d}\tau)$ is caused by the pressure-induced motion of surface A_3; this reduces the resonance frequency of the system and is a destabilizing effect. The term $Z_\xi(\mathrm{d}P/\mathrm{d}\tau)$ is our representation of the control force, by which we wish to improve the system stability.

The linear perturbation equations for the quantities $\delta\phi_1$, $\delta\phi_2$, and $\delta\Psi$, from (9), will become

$$\left.\begin{aligned} \frac{\mathrm{d}\delta\phi_1}{\mathrm{d}\tau} &= B(\Psi'\delta\phi_1-\delta P)-\mu\delta\phi_1, \\ \frac{\mathrm{d}\delta P}{\mathrm{d}\tau} &= \frac{\delta\phi_1-\delta\phi_2}{B}-(\eta+Z_\xi)\frac{\mathrm{d}\delta P}{\mathrm{d}\tau}, \\ \frac{\mathrm{d}\delta\phi_2}{\mathrm{d}\tau} &= \lambda B(\delta P-T'\delta\phi_2). \end{aligned}\right\} \tag{10}$$

These equations are basically identical to (22) and (23) in Epstein *et al.*, but in a form in which the flow acceleration in the throttle duct is considered, and they have solutions of the form $\mathrm{e}^{s\tau}$; equation (10) then reduces to the characteristic equation

$$s^3+a_2s^2+\left[a_1+b_1\left(\frac{1}{1+\eta+\tilde{Z}_\xi}-1\right)\right]\frac{s+a_0}{1+\eta+\tilde{Z}_\xi}=0, \tag{11}$$

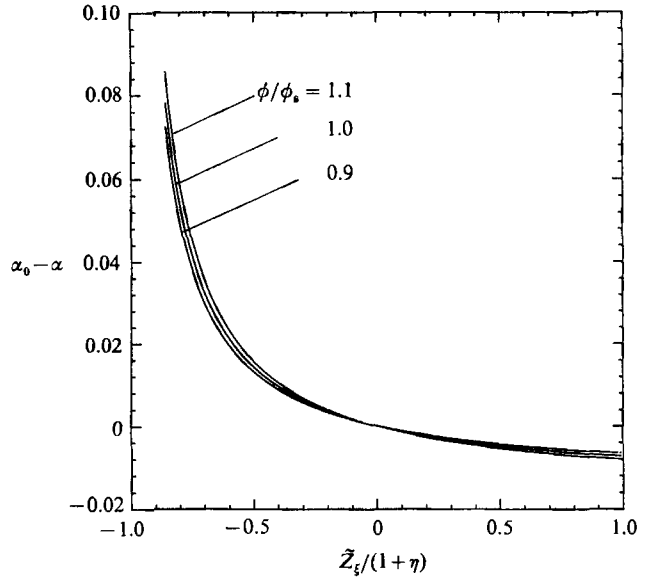

FIGURE 7. The effect of a real control parameter $\tilde{Z}_\xi$ on the system stability. α is the real part of the eigenvalue of equation (11), α_0 being the value when $\tilde{Z}_\xi = 0$. ϕ is the average non-dimensional mass flow, ϕ_s being the value at the natural surge onset point. $(\alpha-\alpha_0) > 0$ indicates the range where the controller stabilizes the compression system.

where a_0, a_1, a_2 have been defined in (6) and $b_1 = 1+\lambda$. $\tilde{Z}_\xi$, generally being a polynomial, or the ratio of two polynomials, in s, is the control law corresponding to applying the operator Z_ξ on $e^{s\tau}$. The control law could also have an exponential term accounting for time delay.

The system stability is now not only dependent on the parameters a_0, a_1, and a_2, but also on the control parameter, $\tilde{Z}_\xi$. The calculated results, carried out around the natural surge point are illustrated in figure 7 for the special illustrative case where $\tilde{Z}_\xi$ is arranged to be real and independent of s. This shows that a real and negative $\tilde{Z}_\xi$ will always improve the system stability in the range $-(1+\eta) < \tilde{Z}_\xi < 0$, while it will tend to destabilize the system when $\tilde{Z}_\xi$ is real and positive. In the absence of a control force ($\tilde{Z}_\xi = 0$), the system stability will be reduced in comparison with that of the hard-walled plenum, because for a spring $\eta > 0$ and η has exactly the same effect on the system stability as does $\tilde{Z}_\xi$, a fact evident from (11). The controller can obviously have a wide range of influence because the control parameter $\tilde{Z}_\xi$ can be arranged to have a variety of complex forms for various complex eigenfrequencies.

In our previous analysis, the compressor and the throttle, which are two nonlinear components in the system, act mainly as energy source and sink. If we stop the rotation of the compressor ($\Psi' = 0$) and close the throttle ($T = 0$, $\lambda = 0$), then the characteristic equation (11) reduces to

$$s^2 + \mu s + \frac{1}{1+\eta+\tilde{Z}_\xi} = 0. \tag{12}$$

We set $\epsilon_0 = 1/(1+\eta)$ and $z = \tilde{Z}_\xi/(1+\eta)$ (these forms are convenient for direct measurement) to write (12) as

$$s^2 + \mu s + \epsilon_0/(1+z) = 0. \tag{13}$$

The control parameter z has the form

$$z = Ge^{i\beta}, \tag{14}$$

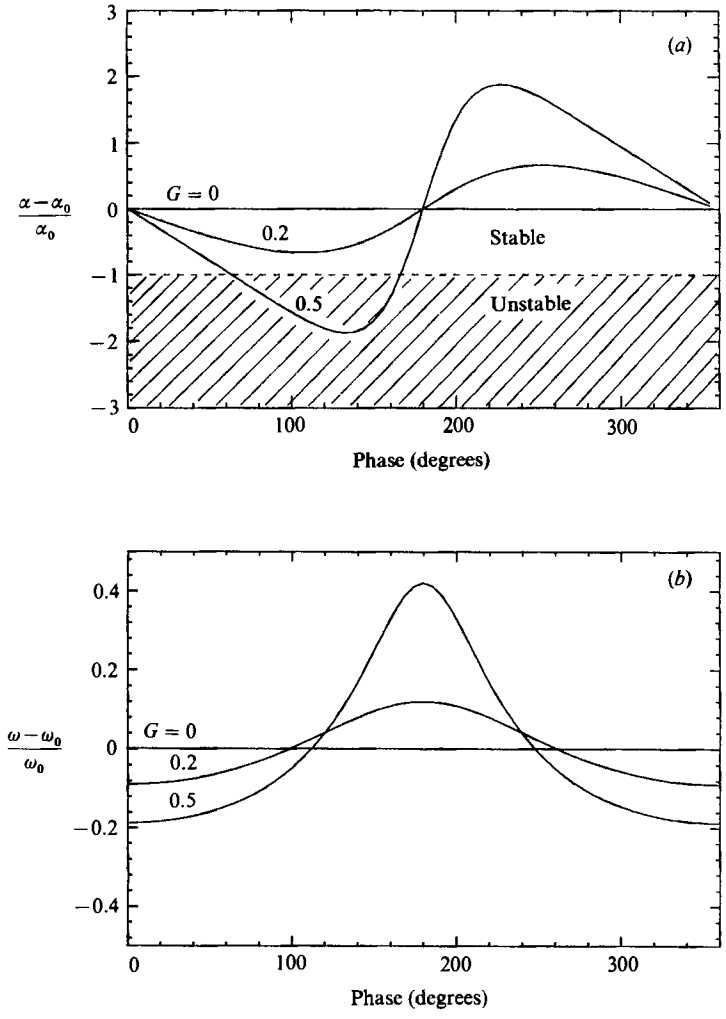

FIGURE 8. (*a*) The system stability is changed by the controlled plenum, depending on the controller gain and the phase shift. (*b*) The system resonance frequency is changed by the controller. α and ω are the real and imaginary parts of the eigenvalue of equation (13), β_0 and ω_0 being the values when $G = 0$.

the gain G and phase β both being real functions of frequency. G is the amplitude ratio of input signal to output signal of the feedback loop and β is the phase-shift in the feedback loop. With no gain ($z = 0$), the solutions of (13) are denoted by

$$s_0 = \alpha_0 \pm \mathrm{i}\omega_0 = -\tfrac{1}{2}\mu \pm \mathrm{i}(\epsilon_0 - \tfrac{1}{4}\mu^2)^{\frac{1}{2}},$$

$\alpha_0 = -\frac{1}{2}\mu$ being the non-dimensional system damping and $\omega_0 \approx \epsilon_0^{\frac{1}{2}}$ (for small damping) the non-dimensional resonance frequency of the uncontrolled system. $\epsilon_0 = 1/(1+\eta) < 1$ because η is positive (the control surface A_3 supported only by the spring reduces the system resonance frequency). We have measured the system resonance frequency, in this condition, to be 28.5 Hz, and on comparing this with the value for the hard-wall plenum, $f_{\mathrm{H}} = 37$ Hz, it follows that $\epsilon_0 \approx 0.6$ and $\eta \approx 0.67$.

The solutions of (13) have a form $s = \alpha + \mathrm{i}\omega$, in which both α and ω are dependent on the control parameter z. We solve (13) and (14) with a constant gain and different

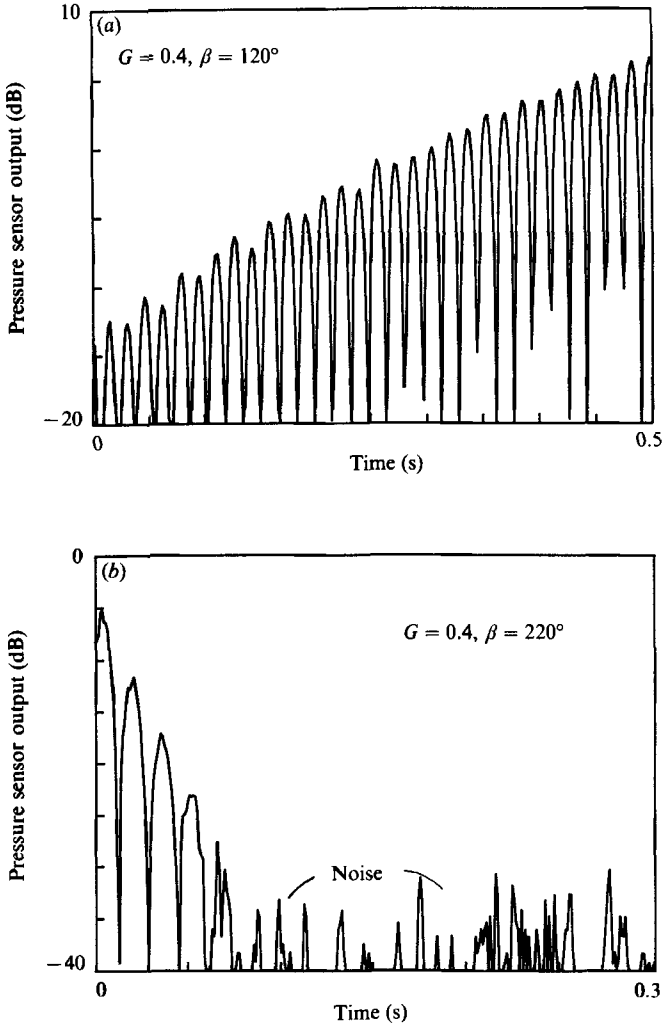

FIGURE 9. (*a*) A typical time history of the system response following the switching on of the controller showing disturbance growth. The phase was set to destabilize an otherwise stable operating condition. (*b*) Temporal response of the system to a pressure impulse – which was damped out quickly. The controller was here set to stabilize a naturally unstable operating condition.

phase shift from 0° to 360°. The calculated results are indicated in figure 8. Figure 8(*a*) shows that in the phase range 0°–180°, the controller will reduce the system damping, even change its sign; while in the phase range 180°–360°, the controller will increase the system damping. From the experimental results in figure 9, we can see these two different trends illustrated. Figure 9(*a*) shows a typical time history of the system response following the switching on of the controller. Figure 9(*b*) shows the impulse response of the system in a case where the controller causes stability.

4. Active stabilization of compressor surge

In our experiments, the effect of the controller on the various aspects of the instabilities and the performance of the compression system were demonstrated by

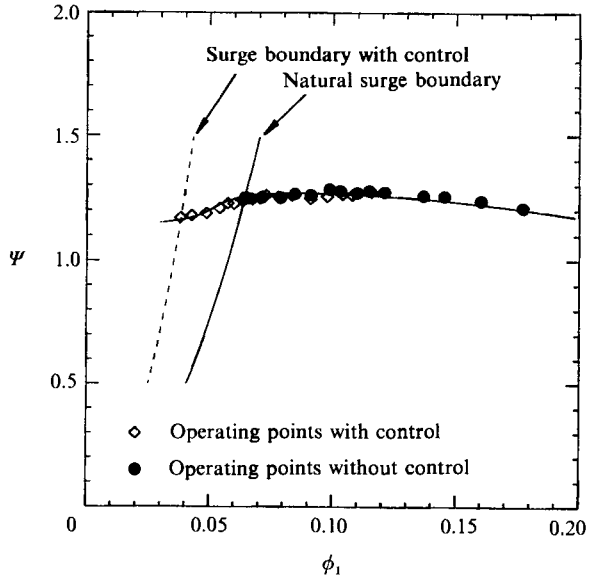

FIGURE 10. The effect of the controller on the compressor performance.

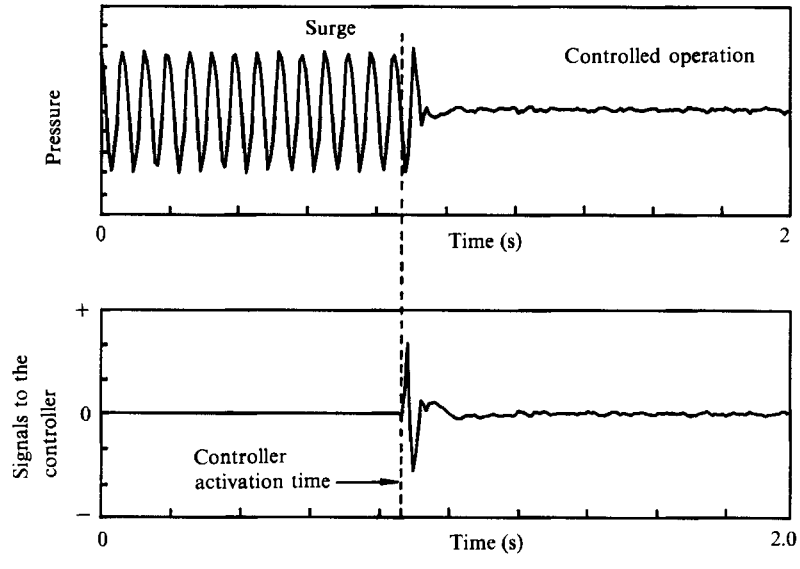

FIGURE 11. Time traces of the pressure fluctuations in the plenum and the signals to the control surface. Surge was completely suppressed following the activation of the controller.

comparing the uncontrolled operation, in which the compression system had a hard-wall plenum, with the controlled operation, in which the plenum had a controllable volume.

The performance of the controlled compression system was assessed in the following ways. First the compressor was operated in the stable region (to the right of the natural surge boundary) with the controller activated. The throttle was then progressively closed to move the compressor operation points towards the natural surge boundary and finally across it, the pressure rise and the mass flow rate being

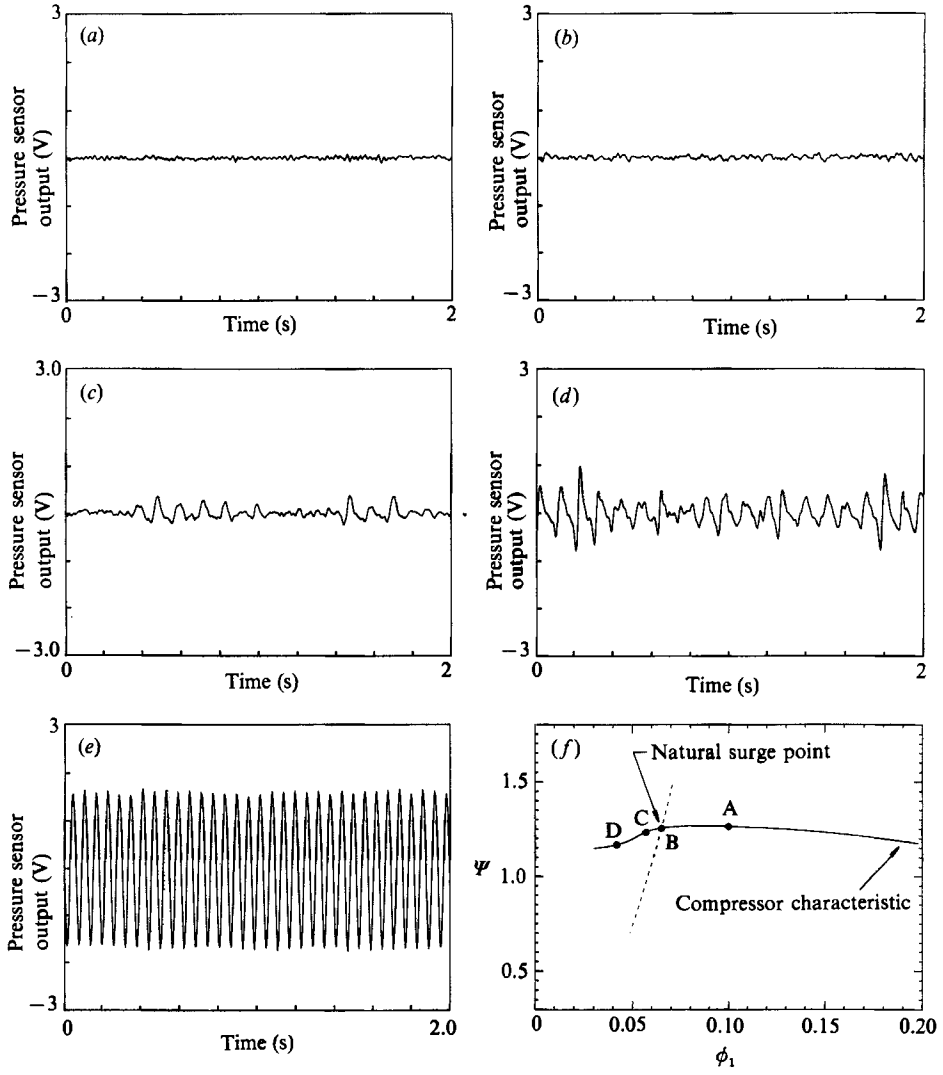

FIGURE 12. Recorded pressure fluctuations in the controlled plenum. A, B, C and D are four operating operating points at which the pressure fluctuations were recorded, (*a–d*) respectively, point A being in the stable operation region while B, C, and D are at points beyond the natural surge boundary. (*e*) shows the surge pressure oscillations at point D when the controller is switched off.

monitored as long as the overall compressor behaviour remained stable. The final throttle position at the point of instability marks the new surge boundary of the controlled compression system. The measured results are illustrated in figure 10, which shows that the controller has made the compression system operate stably beyond its natural surge boundary and in fact moved the surge boundary significantly towards the left.

To observe the effect of the controller on compressor surge, we switched on the controller when the compressor was already operating in deep surge. By deep we mean here that the system is settled into a vigorous and steady oscillation. This is shown in figure 11, where both pressure traces and control signal records are

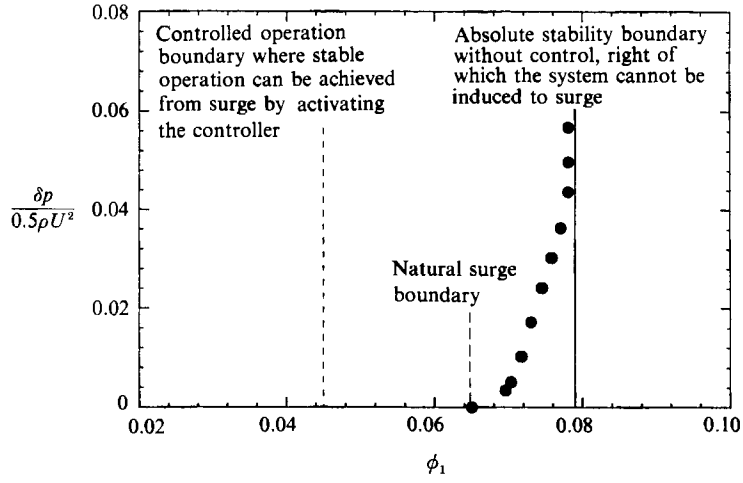

FIGURE 13. Effect of the controller on the stability of the compression system under disturbed operation. The solid line is the experimental stable boundary without control, right of which the system is absolutely free from surge. The dashed line represents a controlled operation position, right of which the controller can effectively suppress an existing surge. The black dots show the level of external disturbance (δp, a sine wave at 20 Hz) that can be tolerated by the uncontrolled system.

illustrated. The controller is extremely effective and the surge is suppressed almost instantaneously. This control effect demonstrates the important fact that the linearly controlled system can recover from surge even though surge is *not* a small-amplitude phenomenon.

As an indication of stability level, we have measured the pressure fluctuations in the plenum while the controlled compressor was operated at different throttle positions. The measured results are given in figure 12. We can see that when the operating point is on the unstable side of the natural surge boundary, the amplitudes of the pressure fluctuations become larger. These pressure fluctuations are not surge (compare figure 12*d* with *e*), but are minor perturbations in a generally steady system. These perturbations are not able to develop into surge because of the action of the controller. In other words, the controller has increased the ability of the compression system to endure external disturbance.

Under normal conditions, to make the compression system surge the throttle should be closed. But that is not a necessary condition. Surge can also be induced by a sufficiently energetic external trigger, even though the system is operated in a linearly stable region. There is a throttle line to the right of the natural surge boundary, beyond which the compression system will not surge under any level of disturbance and is therefore absolutely stable. In our experiments, we measured the stability boundary points under different pressure disturbance levels and took the boundary points corresponding to very large disturbances as that absolutely stable operation line. The measured results are indicated in figure 13, illustrated by black dots. We took the lowest throttle setting at which recovery from surge could be achieved by the controller as the lower stability boundary. This boundary is also indicated in figure 13. Comparing the two stability extremes shows that the controller has greatly enlarged the region of stable operation.

In order to suppress compressor surge, we must correctly choose the control parameter $z = Ge^{i\beta}$, i.e. choose the gain and the phase-shift. Those points, in the

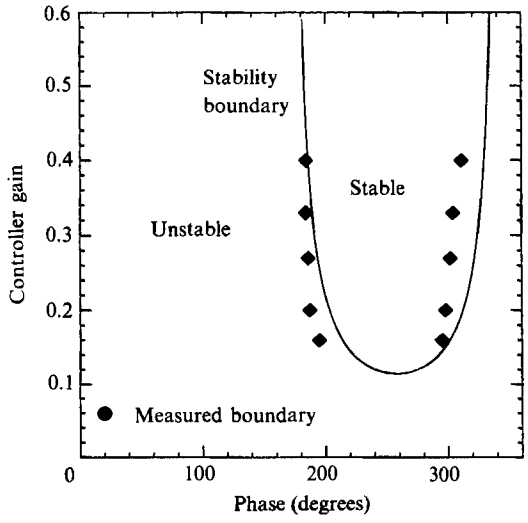

FIGURE 14. The stability map of the compression system with a controlled plenum. The gain is the ratio between the output and the input signals of the feedback loop, while the phase is the phase shift of the two signals. The compressor was operated just left of the natural surge boundary in this example.

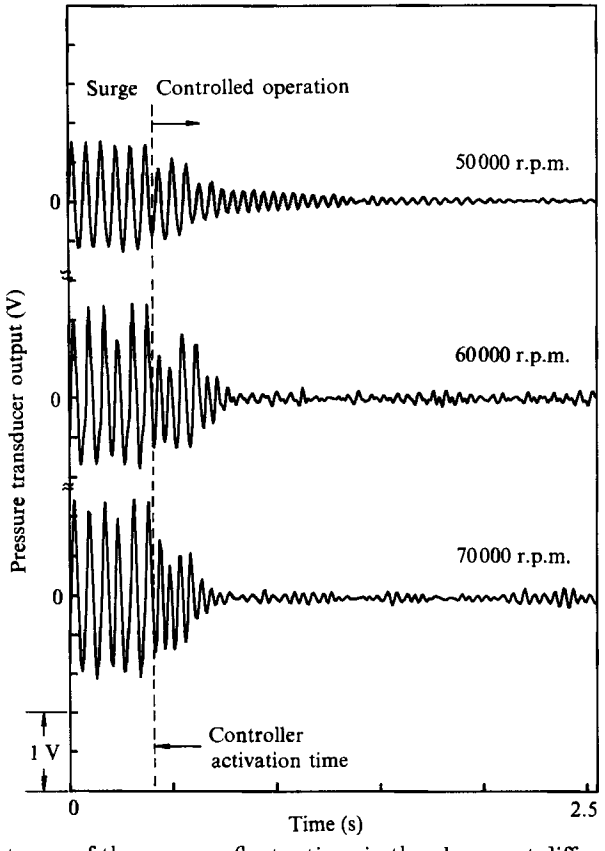

FIGURE 15. Time traces of the pressure fluctuations in the plenum at different speeds following the activation of the controller. The dashed line represents the time at which the controller was switched on. To the left of this line the compressor is in surge; to the right is the subsequent controlled behaviour.

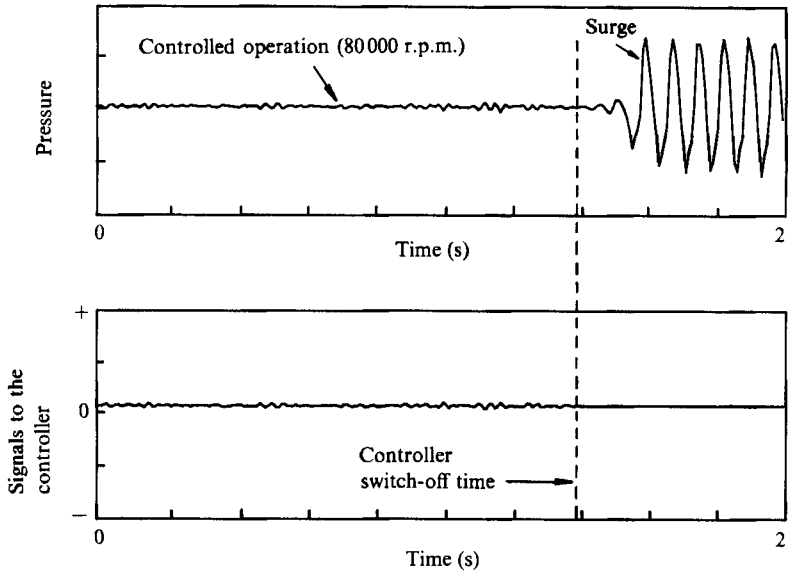

FIGURE 16. Time traces of the pressure fluctuations recorded in the plenum. The compressor was operated at high speed (80000 r.p.m.) and at the surge onset point. Under the influence of the controller the operation was stable; the compressor went into surge immediately after the controller was switched off.

(gain, phase)-plane, at which the controller can suppress surge constitute a stable area, and the points at which the controller cannot suppress the surge (even makes it worse) constitute an unstable region. The two regions are separated by a stability boundary. The controlled-compression-system characteristic equation (11) with a solution $s = \alpha + i\omega$, specifies the stability boundary according to $\alpha = 0$, at which condition we solve (11) at the throttle position just across the natural surge boundary. We thus define the stability boundary and the stable control region on the (phase, gain)-plane. Experimentally, the stability map can be obtained by measuring the effective range of phase angles at various gain settings. A comparison of the theoretical and experimental stability boundaries is mapped out in figure 14. It can be seen that the agreement is good in terms of both trend and location.

We finally examine the behaviour of our controlled compression system at higher rotational speeds (from 50000 to 80000 r.p.m.). The experimental results illustrated in figure 15, which are pressure traces recorded in the plenum following switching on of the controller, show clearly that the controller still has the ability, in the speed range from 50000 to 70000 r.p.m., to bring the system out of the deep surge. When the speed was over 75000 r.p.m., however, we found that the controller became ineffective on the fully developed surge. This is probably because the surge pressure oscillating inside the plenum at this high speed exerts an overwhelmingly strong force on the diaphragm of the loudspeaker and so prevents the control force created by the feedback loop from moving the diaphragm correctly. Since the controller was designed to cancel small disturbances in the early stages of surge development, the controller should still be effective in preventing these initial disturbances from growing, even though the controller will be ineffective once they have developed into surge. This was indeed found to be the case. With the controller switched on thc throttle was closed so as to bring the operating point across the natural surge boundary while maintaining stability. At a suitable point deep enough into the

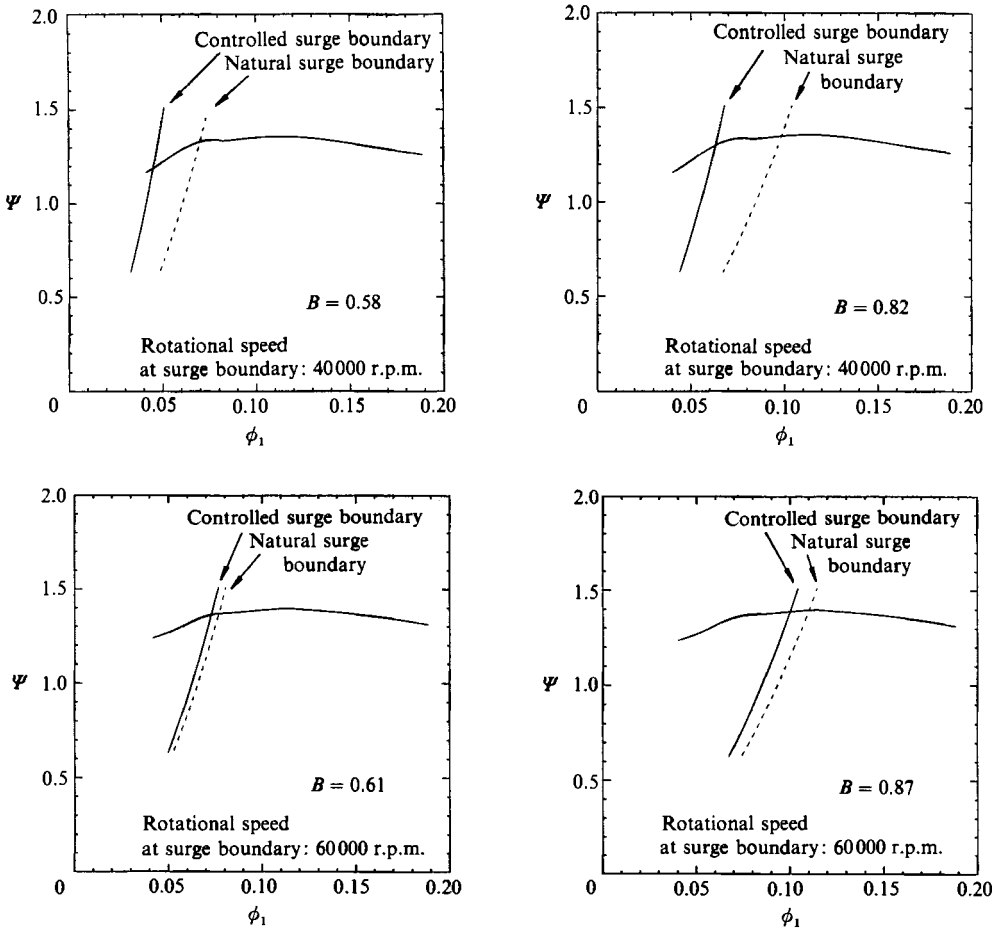

FIGURE 17. The effect of active stabilization on compressor performance at different operation speeds and different parameter B. The position of the natural surge boundary changes as a results of changes in the speeds and in B.

naturally unstable region the controller was switched off and the ensuing collapse into surge was observed. The transient processes are illustrated in figure 16 where surge occurs immediately following the absence of the control action.

The improvement of the surge boundary under controlled conditions was also checked at higher rotational speeds. It was found, by comparing low-speed and high-speed operations as illustrated in figure 17, that the improvement of the surge boundary was always less at high rotational speeds. The lowering of control effectiveness was due to the limited force available in our controller, a force of therefore diminishing non-dimensional strength as the flow increases. The transfer function of the feedback loop is set under a condition where the input signal is small. The motion of our experimental control surface (loudspeaker) is amplitude-limited when the input signal is relatively big, and whenever instability waves get bigger than those which can be generated by the loudspeaker the control becomes improbable. Actuators designed to cope with typical compressor delivery conditions will obviously be different from audio equipment, and the development of those actuators is what is needed now to connect this laboratory demonstration of principle into a useful technology.

5. Conclusions

Active stabilization of compressor surge has been achieved in our experiments with a compression system incorporating a controlled plenum; the controller is able to alter the system damping and the resonance frequency. The results show that the compression system can be effectively stabilized by switching on the controller before or even after surge occurs. Our experiments indicate that the linear controller is effective even in this nonlinear aerodynamic case, and this makes us believe that the stability and the performance of compression systems generally could be greatly improved through active control techniques of this type.

REFERENCES

DORF, R. C. 1980 *Modern Control Systems*, 3rd edn, pp. 148.

EMMONS, H. W., PEARSON, C. E. & GRANT, H. P. 1955 Compressor surge and stall propagation. *Trans. ASME* **79**, 455–469.

EPSTEIN, A. H., FFOWCS WILLIAMS, J. E. & GREITZER, E. M. 1986 Active suppression of compressor instabilities. *AIAA 10th Aeroacoustics Conference Seattle, Paper* 86-1994.

GREITZER, E. M. 1976 Surge and rotating stall in axial flow compressors, part 1: Theoretical compressor model. *Trans. ASME* A: *J. Engng for Power* **98**, 190–198.

GREITZER, E. M. 1981 The stability of pumping systems. *Trans. ASME* I: *J. Fluids Engng* **103**, 193–242.

HANSEN, K. E., JØRGENSEN, P. & LARSEN, P. S. 1981 Experimental and theoretical study of surge in a small centrifugal compressor. *Trans. ASME* I: *J. Fluids Engng* **103**, 391–395.

HUANG, X. Y. 1988 Active control of aerodynamic instabilities. Ph.D. thesis, Cambridge University.

STENNING, A. H. 1980 Rotating stall and surge. *Trans. ASME* I: *J. Fluids Engng*, **102**, 14–20.